p 11

Detecting and Disentangling Nonlinear Structure From Solar Flux Time Series

S. Ashrafi and L. Roszman
COMPUTER SCIENCES CORPORATION (CSC)
Lanham-Seabrook, Maryland, USA*

Abstract

Interest in solar activity has grown in the past two decades for many reasons. Most importantly for flight dynamics, solar activity changes the atmospheric density, which has important implications for spacecraft trajectory and lifetime prediction. Building upon the previously developed Rayleigh-Benard nonlinear dynamic solar model, which exhibits many dynamic behaviors observed in the Sun, this work introduces new chaotic solar forecasting techniques.

Our attempt to use recently developed nonlinear chaotic techniques to model and forecast solar activity has uncovered highly entangled dynamics. This paper presents numerical techniques for decoupling additive and multiplicative white noise from deterministic dynamics and examines falloff of the power spectra at high frequencies as a possible means of distinguishing deterministic chaos from noise that is spectrally white or colored. The power spectral techniques presented are less cumbersome than current methods for identifying deterministic chaos, which require more computationally intensive calculations, such as those involving Lyapunov exponents and attractor dimension.

1. Introduction

1.1 Review of Solar Activity

Need for Solar Flux Prediction. Solar flux $F_{10.7}$ [radio flux emitted at a wavelength of $\lambda = 10.7$ centimeters (cm)] is the best indicator of the strength of ionizing radiations, such as solar ultraviolet and X-ray emissions, that directly affect the atmospheric density and thereby change the orbit lifetime of satellites. Thus, accurate forecasting of solar flux $F_{10.7}$ is crucial for spacecraft orbital determination.

Sunspots and Solar Flux. The strong correlation between sunspots and the solar flux $F_{10.7}$ is probably due to the enhanced radiation from limited areas of the Sun where sunspots are active.

The dynamics of sunspots and their formation is still a mystery. They are often more than 1000 degrees Kelvin cooler than the surrounding photosphere. Although many explanations for sunspot cooling have been proposed (e.g., the Biermann field inhibition mechanism and the superadiabatic downflow mechanism), the huge difference in temperature between sunspots and their surroundings suggests a similarity with solitons of multilevel turbulence. One may think of sunspots as solitons in a fluid turbulent Sun. Orbit lifetime is a function of atmospheric drag, which is a function of atmospheric density, which in turn is a function of solar flux. For this reason, spacecraft orbit determination requires accurate forecasting of solar flux.

Nonlinear Structure in Solar Flux. Until recently, we had little reason to doubt that weather is in principle predictable, given enough data. Recently, a striking discovery changed our perspective: simple deterministic systems with only a few degrees of freedom can generate random behavior. When a system exhibits apparent random behavior that is fundamental to its dynamics, such that no amount of information gathering will make the system predictable, the system is considered to be chaotic. Much evidence supports our assertion that solar flux signal falls in this category.[1, 2] Perhaps paradoxically, chaos is generated by fixed rules that do not in themselves involve any element of chance. Theoretically, the future of a dynamic system is completely determined by present and past conditions. In practice, however, amplification of small initial uncertainties makes a system with short-term predictability unpredictable in the long term.

Many people speak of random processes as though they were a fundamental source of randomness. This idea is

* This work was supported by the National Aeronautics and Space Administration (NASA)/Goddard Space Flight Center (GSFC), Greenbelt, Maryland, Contract NAS 5-31500.

(NASA-CR-190510) DETECTING AND DISENTANGLING NONLINEAR STRUCTURE FROM SOLAR FLUX TIME SERIES (Computer Sciences Corp.) 11 p

N92-28871

Unclas

G3/92 0106531

misleading. The theory of random processes is an empirical method to deal with incomplete information; it does not attempt to explain randomness. As far as we know, the only truly fundamental source of randomness is the uncertainty principle of quantum mechanics; everything else is deterministic, at least in principle. Nonetheless, we call many phenomena, such as solar dynamics, random, even though we may not ordinarily think of them in terms of quantum mechanics. Historically, scientists have assumed that randomness derives solely from complication. In this paper, we will take the practical position that randomness occurs to the extent that a system's behavior is unpredictable. We believe that randomness is subjective and a matter of degree; that is, some systems are more predictable than others (e.g., solar activity is more predictable than geomagnetic activity).

Solar Activity Prediction. Interest in solar activity has grown in the past two decades for many reasons. Some reports claim a correlation between solar activity and weather on Earth, although a correlation has not yet been convincingly established. We have some evidence for the coincident occurrences of the Maunder minimum (a period of little or no solar activity occurring from 1645 to 1715) and the "Little Ice Age" (a period of abnormally cold weather). Perhaps most importantly for flight dynamics, solar activity changes the atmospheric density, which has important implications for spacecraft trajectory and lifetime prediction.[3] The seemingly random nature of solar flux has misled us for many decades, causing us to assume that the underlying physics must necessarily be complex as well. Therefore, researchers have generally used statistical models to predict solar activity.[4] However, new developments in chaos and nonlinear dynamics allow us to model the behavior of a system in terms of some invariants directly extractable from system dynamics, without reference to any underlying physics. Using chaos theory, we can predict short-term activity more accurately than with statistical methods; however, chaos theory imposes a fundamental limit on long-term predictions.

1.2 Brief Review of Nonlinear Dynamics

Self-Organization and Attractors. Imagine a very simple system: a pendulum. The pendulum exhibits two fundamental degrees of freedom: position and momentum. However, in its stable periodic state (limit cycle), the pendulum can be described by only one degree of freedom, the phase angle. Here, the dynamic is attracted to a lower-dimensional phase space, and the dimension of this reduced phase space is equal to the number of active degrees of freedom in the self-organized system.

Attractors are not limited to zero dimension (fixed point) or one dimension (limit cycle), but for nonlinear systems they could be high dimensional and in some cases even fractional or fractal (strange attractors).

Phase-Space Construction Directly From a Time Series. When confronted with a complicated physical system, an experimenter normally measures at regular and discrete intervals of time the value of some state variable (e.g., flux $F_{10.7}$) and records the time series $f(t_0), f(t_1), f(t_2),\ldots$, with $f(t_i) \in R$ and $t_i = t_0 + i\Delta t$. From the observed time series, the experimenter attempts to infer something about the dynamics (i.e., the physics) of the system.

From time-delayed values of the scalar time series, Packard et al.[5] have shown that one can embed the time series into a higher dimensional space. Vectors are created with components as

$$\vec{f}(t) = [f(t),\ f(t-\tau),\ \ldots\ f(t-(m-1)\tau)]^T,$$

where τ (time delay) and m (the embedding dimension) are parameters of the embedding procedure.

An embedding dimension of $m > 2D+1$, where D is the fractal dimension of the attractor, almost always ensures the construction of the topology of the attractor (Takens' theorem).

If unlimited infinitely precise data are available, almost any delay time τ and embedding dimension $m > D$ will work, at least in principle. However, choosing the optimal parameters for real data is a nontrivial process.

For example, if τ is too large, then the components f(t) and $f(t + (m-1)\tau)$ of the reconstructed vector will be effectively uncorrelated, which will inflate the estimated dimension. On the other hand, if $(m-1)\tau$ is too small, then the components $f(t), \ldots, f(t+(m-1)\tau)$ will all be very nearly equal, and the reconstructed attractor will look like one long diagonal line. Generally, τ must not be less than some characteristic decorrelation time, and $(m-1)\tau$ must not be much greater than this decorrelation time. One such characteristic time is the local minima of the autocorrelation function.

Largest Lyapunov Exponent of Solar Flux Time Series. The sum of the Lyapunov exponents is the time-averaged divergence of the phase-space trajectory; hence, any dissipative dynamical system will have at least one negative exponent.

A small positive Lyapunov exponent is an indication of chaos, and a very large positive Lyapunov exponent is an indication of a totally stochastic or random system. Therefore, the sign of the exponent provides a qualitative picture of a system's dynamics—a positive exponent represents chaos, a zero exponent represents marginally stable systems, and a negative exponent represents periodic systems. The largest Lyapunov exponent for solar activity is about 0.01.[2, 5] There, we have used the well-known technique of phase-space reconstruction with delay coordinates.[6]

Toward Forecasting Solar Flux Directly From Its Time Series. After embedding the solar flux time series in a state space using the Takens-Packard delay coordinate technique, one can "learn" the induced nonlinear mapping using a local approximation. This will allow us to make short-term forecasting of the future behavior of our time series using information based only on past values. The error estimate of such a technique has already been developed by Farmer and Sidorowich[7]:

$$E \approx Ce^{(m+1)KT} N^{-(m+1)/D},$$

where E: normalized error of prediction ($0 \leq E \leq 1$, where zero is perfect prediction, and one is a prediction no better than average)

m: order of local approximation

K: Kolmogorov entropy

T: forecasting window

N: number of data points

D: dimension of the attractor

C: normalization constant.

Using the Farmer-Sidorowich relation, we can find the prediction horizon T for the zeroth order of local approximation. Any prediction above T_{max} is no better than average constant prediction:

$$E(T_{max}) = 1.$$

Thus, for m = 0, K is the largest Lyapunov exponent λ. Therefore,

$$e^{KT_{max}} N^{-1/D} \sim 1 \quad \text{or} \quad T_{max} \sim \frac{\ln (N)}{KD},$$

$$T_{max} \sim \frac{\ln (N)}{\lambda D}$$

Any prediction beyond the indicated horizons is no better than average value. The connection between the local and the global Lyapunov exponents has recently been found by Abrabanel and Kennel (March 1991) in a form of power law as

$$\lambda(l) = \lambda_G + \frac{c}{l^v},$$

$$N = \omega l,$$

where $\lambda(l)$ = local Lyapunov exponent

l = length of observed data (observation window)

v = a constant dependent to the dynamical system ($0.5 \leq v \leq 1.0$)

c = a constant dependent to initial conditions of the system

λ_G = well-known global Lyapunov exponent

ω = frequency of data points.

Because all data are of finite length, using the Abrabanel-Kennel power law and Farmer-Sidorowich relation, we can find T_{max} as

$$T_{max} \sim \frac{\ln(l\omega)}{\left(\lambda_G + \frac{c}{l^v}\right) D}.$$

This means that as l increases linearly, T_{max} increases logarithmically to a certain asymptotic T because of the denominator c/l^v.

Therefore, our relation shows that at the asymptote $T_{max} = T_0$ and $dT_{max}/dl = 0$.[7] Thus, we can find what observation window is required for forecasting up to T_{max} within some confidence level:

$$\frac{dT_{max}}{dN} \rightarrow 0, \text{ thus } N_0 \sim e^{\frac{x_0(\delta)}{v}}, \; x_0(\delta) > 2,$$

where $x_0(\delta)$ is the solution to $e^{-x}(x-1) = \delta$, and where

$$\delta = \frac{\lambda_G}{c\omega^v}$$

is the scaled global Lyapunov exponent.

This result shows that any observation window greater than $l_0 = N_0/\omega$ will not improve our prediction horizon T_0; so more data beyond this limit are not needed to understand a dynamical system. This conclusion is indeed consistent with weather prediction and also with empirical results concluded from neural networks training.

1.3 Analysis of High-Frequency Power Spectra of a Time Series

Figure 1 shows daily solar flux $F_{10.7}$ for four solar cycles of about 11.5 years (from February 1947 to November 1991). From the graph, it is clear that some long-term features show a higher degree of order than some short-term features. For example, 11.5-year solar cycles are less stochastic than daily variations. Therefore, it seems that one may be able to simulate solar dynamics using only a few degrees of freedom.

It is also clear from Figure 1 that variation of daily activity for solar cycle maxima is greater than for solar cycle minima. The flux on the maxima varies by as much as 150 solar flux units, whereas on the minima the flux varies by no more than 25 units. To simulate this phenomenon, we require a long-term variation $X_L(t)$, a medium-term variation $X_M(t)$, and a short-term variation $X_S(t)$. We therefore assert that solar activity may be simulated with three degrees of freedom. In this paper, we attempt to elucidate the inherent structure in these different time scales and to show that, from the falloff of the power spectra of each of these variations at high frequencies, one can deduce whether the signal is chaotic. The power spectral techniques presented are less cumbersome than current methods for identifying deterministic chaos, which require more computationally intensive calculations, such as those involving Lyapunov exponents and attractor dimension.

Historically, random behavior in systems has been studied as an effect of noise, (e.g., Brownian motion). With the emergence of chaos theory, we began to understand that random behavior can occur intrinsically in deterministic systems even if the number of degrees of freedom is small. Recognizing these two sources of random behavior, it is obviously crucial that we be able to determine which is the cause in a given case. That is, we must know whether the observed random behavior can be described by a small number of deterministic equations or is more accurately modeled by a stochastic process. We attempt to provide a partial answer to this fundamental question.

With our current understanding of chaotic dynamics, we can calculate the fractal Hausdorff dimension of attractors, determine the positive Lyapunov exponents, and thereby distinguish deterministic chaos from stochasticity. These methods, however, involve many well-known technical difficulties when applied to time series data.[7] What is needed is a tool that allows us to distinguish between deterministic and stochastic random behavior without first calculating Lyapunov exponents, dimensions, and entropies. We attempt to show that the falloff of the power spectra at high frequencies and Hilbert transform of our data can furnish such a tool. Our results indicate that systems that can be described by deterministic chaos with a few degrees of freedom should have power spectra that fall off exponentially and that the stochastic system should decay via a power law.

Consider f(t), a time series that is either stochastic or chaotic. Let $F(\omega) = \mathcal{F}\,[f(t)]$ be a Fourier transform of f(t). If f(t) is differentiable with respect to time, the Fourier transform of df/dt is: $\omega\ F(\omega)$. Thus, if $F(\omega)$ exists, $F(\omega)$ must fall off faster than ω^{-1} as $\omega \to \infty$, so that the inverse transform of $i\omega\ F(\omega)$ will exist. Now, the power spectrum of f(t), $S_f(\omega)$, is, roughly, $S_F(\omega)\ \alpha\, |F(\omega)|^2$. It follows that if f(t) is once differentiable, $S_f(\omega)$ must fall off faster than ω^{-2}. Similarly, if the nth derivative of f(t) exists, then $S_f(\omega)$ falls off faster than ω^{-2n}. For model systems like the Lorenz model, one may expect the power spectra of a dynamical system to fall off faster than any power of ω^{-1}.

2. Data Analysis

Using interpolation and decimation one can decouple solar flux time series to three (the dimension of embedding space) variables, all functions of time. These three variables are $X_L(t)$, long-term behavior; $X_M(t)$, medium-term behavior; and $X_S(t)$, short-term behavior.

Increasing the Sample Rate of Data. First, we expand the input time series in length by inserting zeros between the original data values. Second, we design a special symmetric finite-duration impulse response (FIR) filter that allows the original data to pass through unchanged and interpolates between data points to minimize the mean-square errors between the interpolated points and their ideal values. Finally, we apply the filter to the input vector to produce the interpolated output vector.

This technique, the opposite of decimation, can increase the sample rate of signal data.

Decreasing the Sample Rate of Data. Decimation, the opposite of interpolation, can decrease the sample rate of signal data. First, we low-pass filter the input time series, and the resulting smoothed signal is resampled at a lower rate. Second, we filter the input time series using an eighth-order low-pass Chebyshev type I filter in both the forward and reverse directions to remove all phase distortion, which effectively doubles the filter order. Orders above 13 produce numerical instability. Third, we take the normalized cutoff frequency for the low-pass filter to be 0.8/r (r is the sample rate), with 0.05 decibels of ripple in the passband.

Finally, we resample the filtered data with low sampling rate.

3. Numerical Techniques For Forecasting Solar Activity

Once we know the state space representation, the next goal is to fit a model to the data. There are several methods. The simplest method is to assume that the dynamics can be written as a map in the form

$$f_{n+1} = M(f_n),$$

where the current state is f_n, and f_{n+1} is a future state. Methods such as the polynomial method, rational approximation, radial basis functions, neural networks, and local approximations have been proven successful. Here we only introduce local approximation technique, which is the method used to structure the computer program.

Local Approximation. The basic idea is to break up the domain of M into local neighborhoods and fit different parameters into each neighborhood. This fit is generally better than global approximation, especially for large data sets. Most global representations reach a point of diminishing returns, where adding more parameters or data gives only an incremental improvement in accuracy. After a certain point, adding more local neighborhoods is usually more efficient than adding more parameters and going to higher order. With local approximation, it is possible to use a given functional representation efficiently. The key is to choose the local neighborhood size correctly, so that each neighborhood has just enough points to make the local parameter fits stable.

An example of local approximation is *first order*, or *nearest neighbor*, approximation. Look through the data set for nearest neighbor, and predict the current state based on what the neighbor did at time T later. We approximate $f(t + T)$ by $f(t, T) = f(t' + T)$, where $f(t')$, is the nearest neighbor of $f(t)$. That is, to predict tomorrow's solar flux, we would search the historical record and find the solar flux pattern most similar to that of today, and predict that tomorrow's solar flux pattern will be the same as the neighboring pattern 1 day later. First order approximation can sometimes be improved by finding more neighbors and merging their predictions, for example, by weighting according to distance from the current state.

Implementation of Local Approximation. Finding neighbors in a multidimensional data set is time consuming when considering many points. A straightforward method is to compute the distance to each point, which takes approximately N steps for N points. This can be reduced to roughly log N steps by organizing the data with a decision tree, such as a $k-d$ tree.[8]

In this method, the data set is partitioned one coordinate at a time. We can take the coordinate with largest range and partition it at its median value. These values are stored in the tree as *keys*. It is now possible to eliminate many points from consideration when looking for the nearest neighbors. This way, we minimize processing time considerably.

3.1 Using Three Degrees of Freedom to Describe and Forecast Solar Flux

As described in Section 1.3, we can decouple solar flux time series to a long-term behavior, X_L, a medium-term behavior, X_M, and a short-term behavior, X_S. Figure 4 shows the long-term behavior, and Figure I shows the combined medium-term and short-term behaviors. The combined behavior looks like a modulated signal (two signals multiplied to one another). Going through some logarithmic decomposition techniques and filtering, one can get the individual medium-term and short-term behaviors shown in Figures 7 and 10, respectively.

Figures 2, 5, 8, and 11 show the Hilbert transform of solar activity for Figures 1, 4, 7, and 10, respectively. This transformation returns a complex sequence; it has a real part (horizontal axis), which is simply the original data, and an imaginary part (vertical axis), which contains the Hilbert transform. The imaginary part is a version of the original real sequence with a 90° phase shift. The Hilbert transformed series has the same amplitude and frequency content as the original real data and includes phase information dependent on the phase of the original data. Figures 3, 6, 9, and 12 show the power spectral density with 95 percent confidence estimation for Figures 1, 4, 7, and 10, respectively. From the form of these decays (in frequency) it is clear that one can distinguish whether the data are stochastic ($\omega^{-\beta}$ decay) or chaotic ($e^{-\alpha\omega}$ decay).

From Figures 5 and 8 it is clear that X_L and X_M follow very distinct trajectories, whereas X_S in Figure 11 is truly stochastic with no distinct trajectory. Therefore, using three degrees of freedom, one can forecast solar activity using chaotic dynamics better than using stochastic methods.

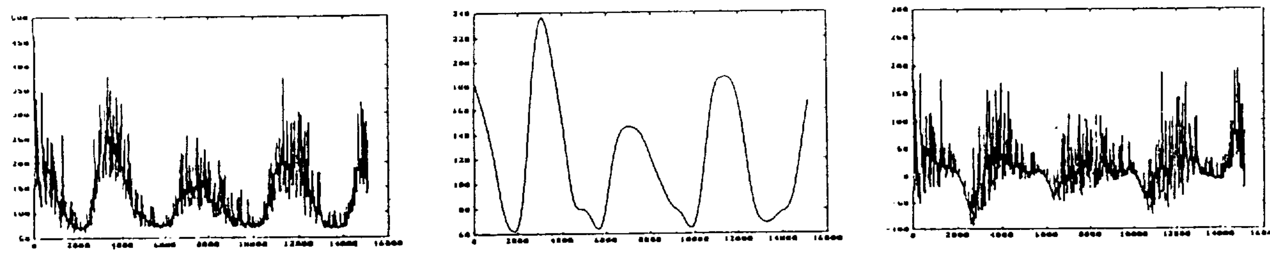

Fig. I. Daily Solar Flux, Its Envelope, and Their Difference

Figures 13 and 14 show predictions using local approximation technique. Figure 15 shows the difference in predictions for embedding dimension D = 3 at different time shifts.

4. Conclusion

In this paper, we have introduced nonlinear techniques to model and forecast solar activity. Signal analysis suggested that although solar flux exhibits highly entangled dynamics, one can use chaos theory to forecast the activity using only a few degrees of freedom.

In view of the difficulty in identifying a stochastic signal from a chaotic one, we also introduced falloff of power spectra at high frequencies as a possible means of distinguishing deterministic chaos from noise that is spectrally white or colored. This power spectral technique is less cumbersome than current methods for identifying deterministic chaos which require more computationally intensive calculations, such as those involving Lyapunov exponents and attractor dimension.

5. References

1. Ashrafi, S., and L. Roszman, "Evidence of Chaotic Pattern in Solar Flux Through a Reproducible Sequence of Period-Doubling-Type Bifurcations," *Proceedings of Flight Mechanics/Estimation Theory Symposium*, National Aeronautics and Space Administration, Goddard Space Flight Center, May 1991

2. Ashrafi, S., and L. Roszman, Computer Sciences Corporation (under contract to Goddard Space Flight Center, Flight Dynamics Division), *Limits on the Predictability of Solar Flux Time Series*, Proceedings of 1st Experimental Chaos Conference, June 1991

3. Walterscheid, R. L., "Solar Cycle Effects on the Upper Atmosphere: Implications for Satellite Drag," *J. Spacecraft*, *26*, 1989

4. Withbroe, G. L., "Solar Activity Cycle: History and Predictions," *J. Spacecraft*, 26, 1989

5. Ashrafi, S., Goddard Space Flight Center, Flight Dynamics Division, prepared by Computer Sciences Corporation, 554-FDD-91/125, *Future Missions Studies: Combining Schatten's Solar Activity Prediction Model With a Chaotic Prediction Model*, November 1991

6. Packard, N., et al., "Geometry From a Time Series," *Phys. Rev. Lett.*, *45*, 1980

7. Farmer, J., and J. Sidorowich, "Predicting Chaotic Time Series," *Phys. Rev. Letts.*, *59*, 1987

8. Bentley, J. H., "Multidimensional Binary Search Trees in Data Base Applications," *IEEE Transactions on Software Engineering*, 5(4), 1979

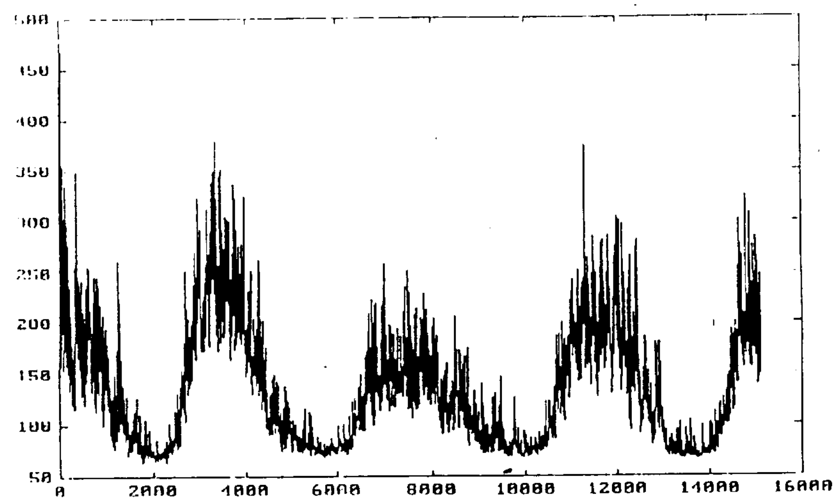

Fig. 1. Daily Solar Flux From 1947 to 1991

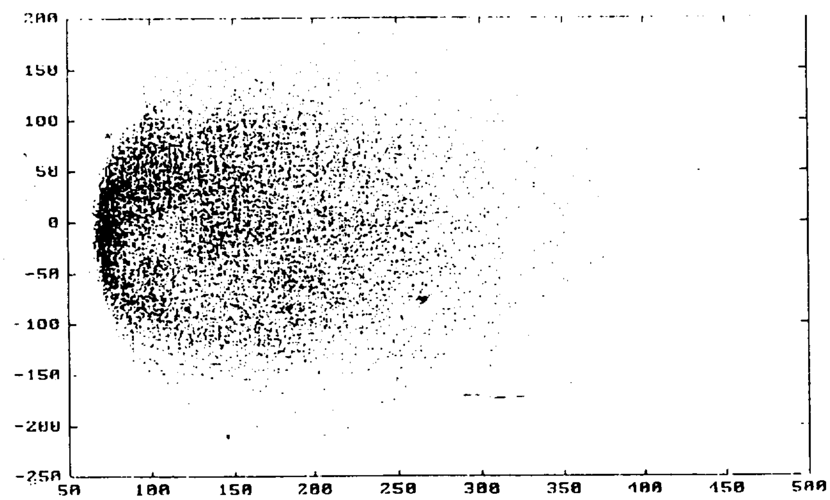

Fig. 2. Hilbert Transform of Fig. 1 Versus Solar Flux

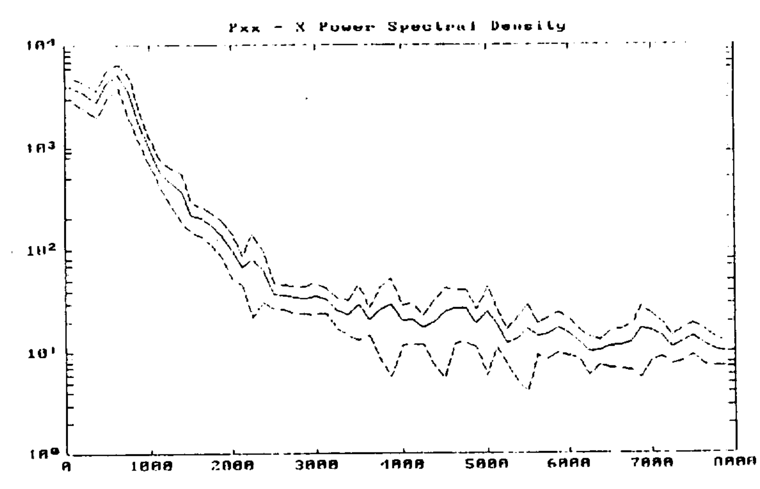

Fig. 3. Power Spectra of Fig. 1 With 95% Confidence Levels

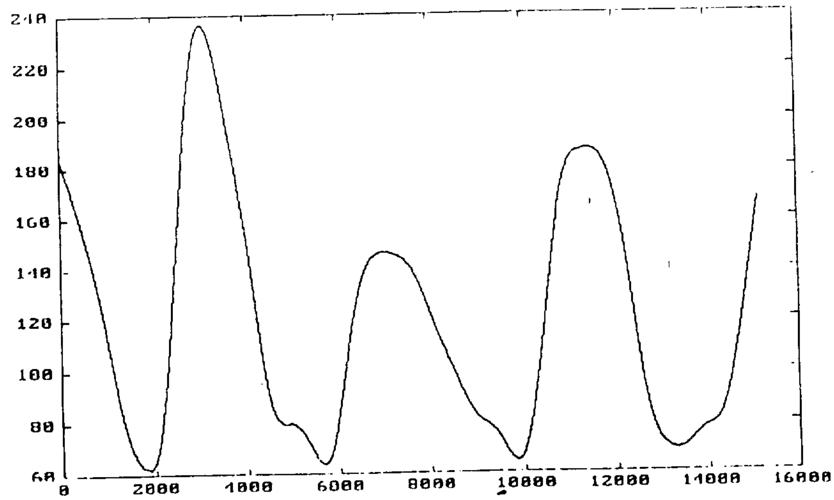

Fig. 4. Long-Term Behavior of Fig. 1.

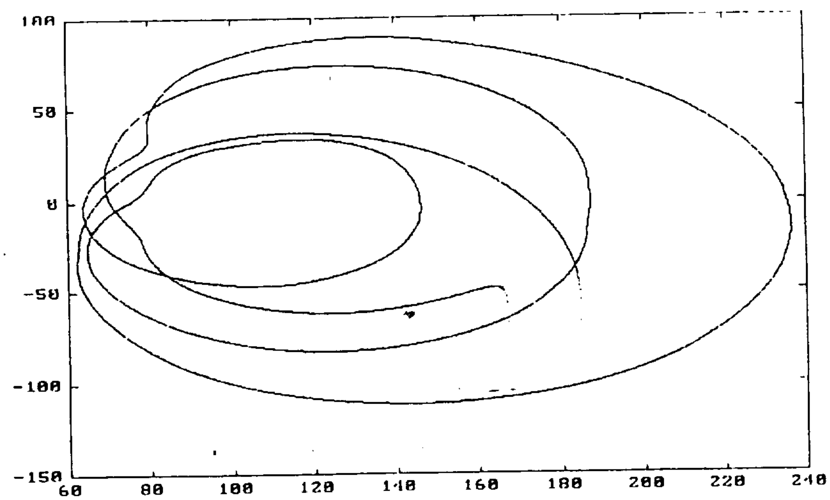

Fig. 5. Hilbert Transform of Fig. 4 Versus Solar Flux

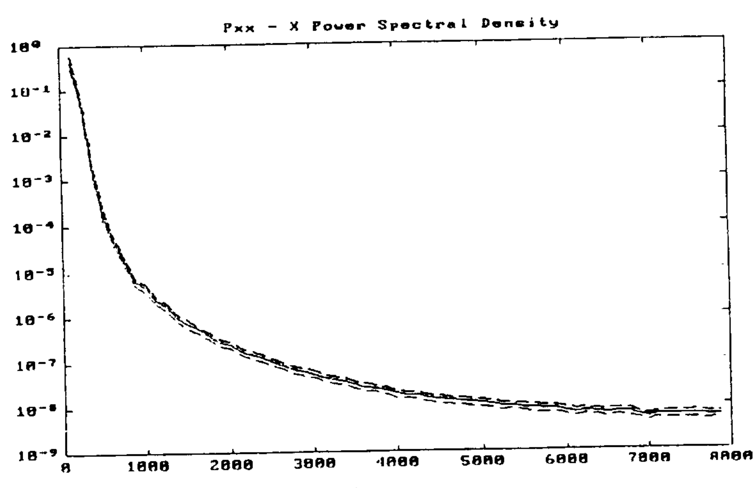

Fig. 6. Power Spectra of Fig. 4 With 95% Confidence Levels

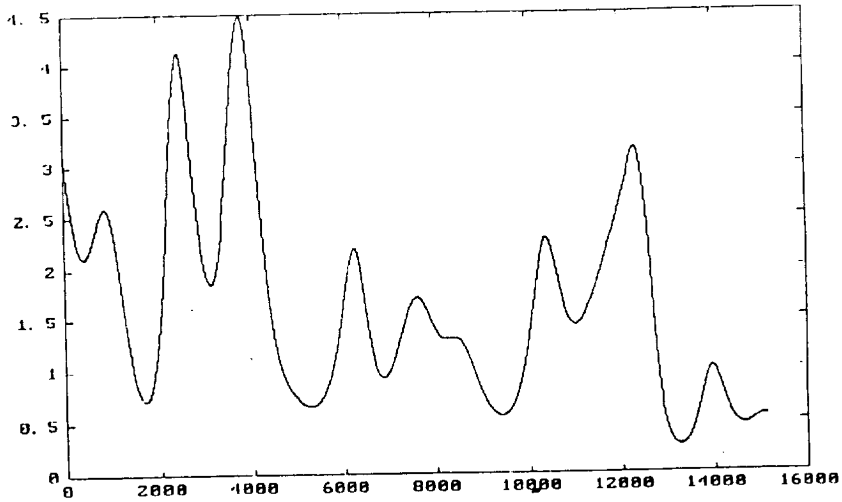

Fig. 7. Medium-Term Behavior of Fig. I

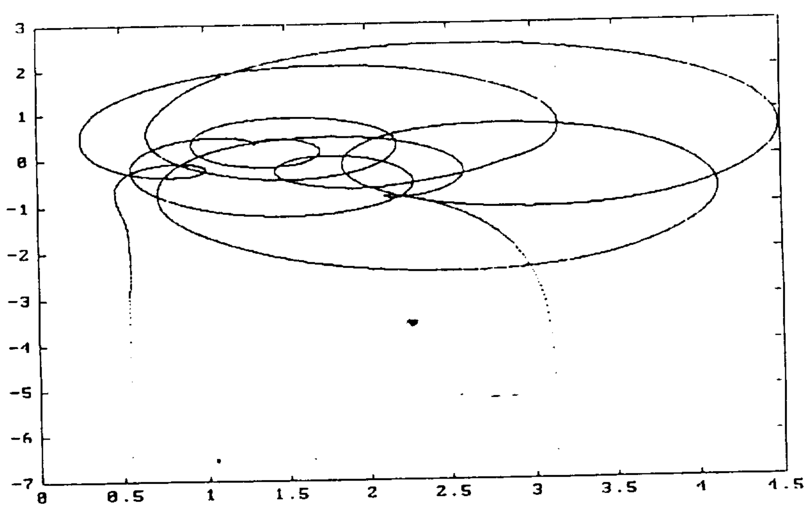

Fig. 8. Hilbert Transform of Fig. 7 Versus Solar Flux

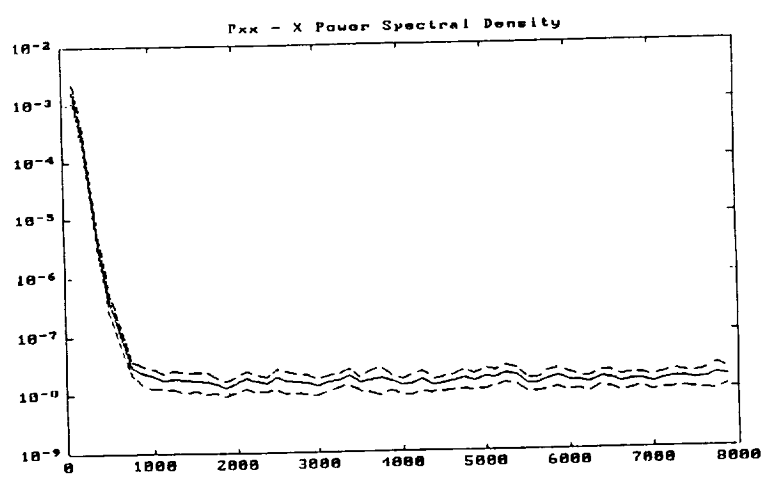

Fig. 9. Power Spectra of Fig. 7 With 95% Confidence Levels

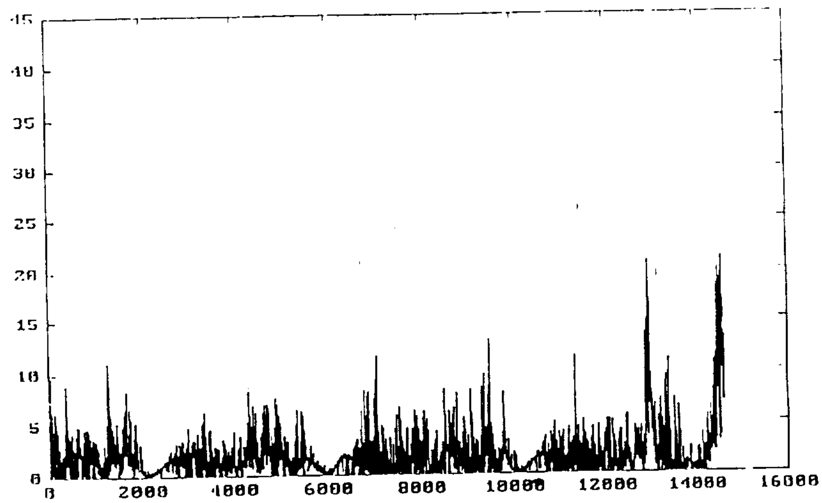

Fig. 10. Short-Term Behavior of Fig. I

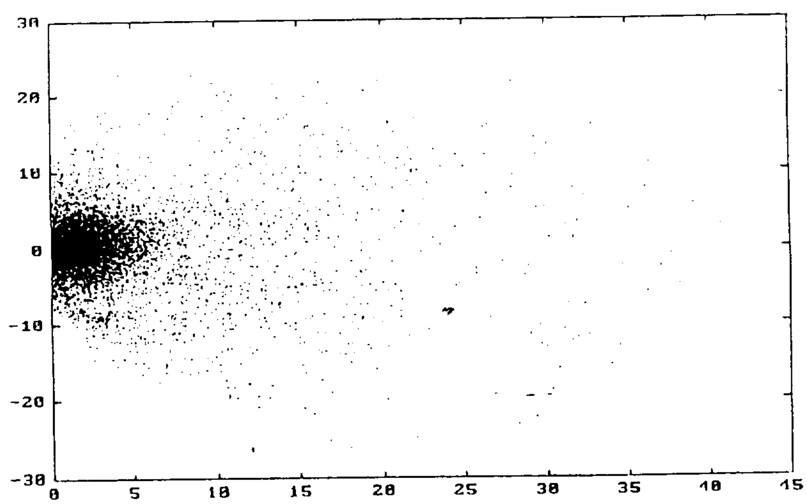

Fig. 11. Hilbert Transform of Fig. 10 Versus Solar Flux

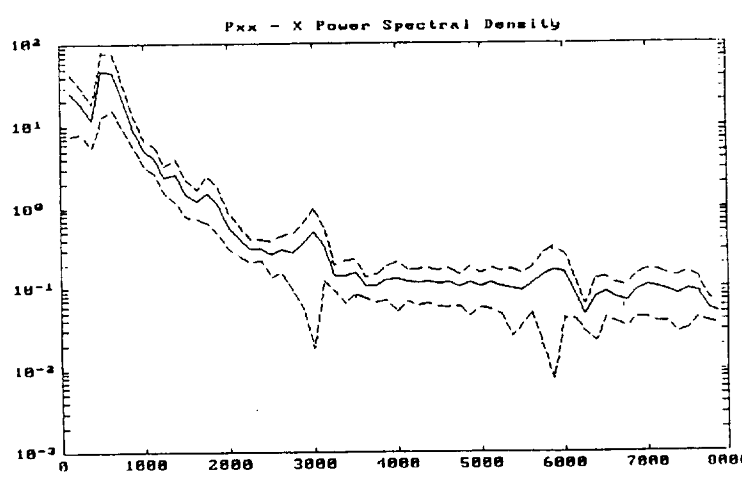

Fig. 12. Power Spectra of Fig. 7 With 95% Confidence Level

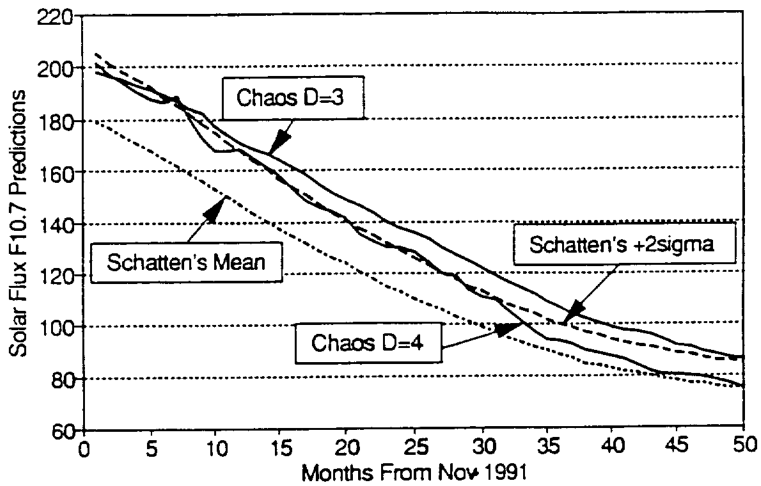

Fig. 13. Predictions of Chaos Theory Compared With Schatten

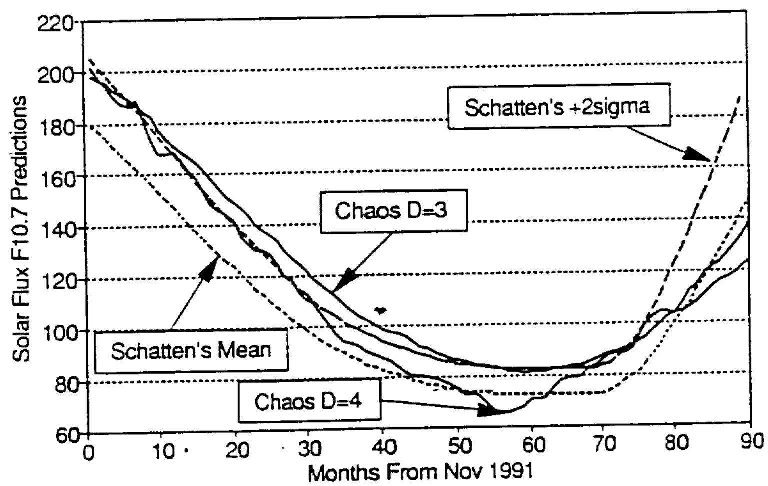

Fig. 14. Predictions of Schatten and Chaos Theory for Minima

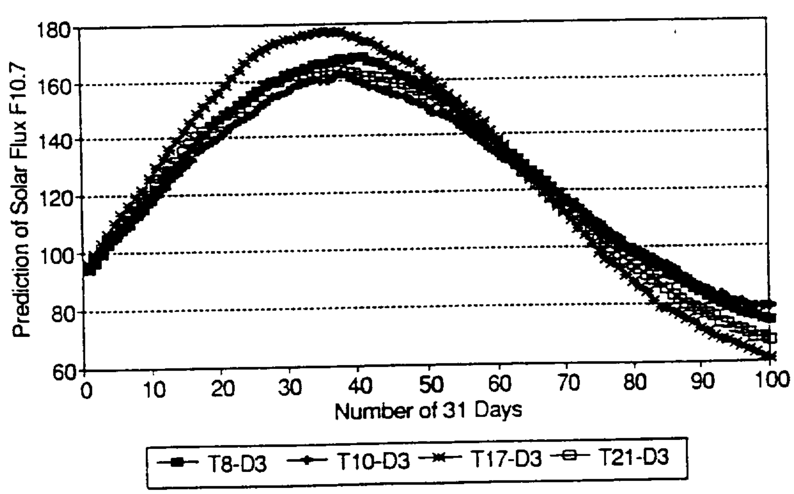

Fig. 15. Variations of Predictions With Changes in Time Shift